



# Flow routing with unknown rating curves using a state-space reservoir-cascade-type formulation

Jozsef Szilagyi<sup>\*,1</sup>, Gabor Balint, Balazs Gauzer, Peter Bartha

*National Hydrological Forecasting Center, VITUKI, Hungary*

Received 10 December 2003; revised 10 January 2005; accepted 24 January 2005

## Abstract

A discrete version of the Kalinin–Milyukov–Nash-cascade is formulated for operational forecasting of stream stages when no information of rating curves is available. Model performance is slightly reduced in comparison to flow routing results using accurate, single-valued stage-discharge relationships. However, when only inaccurate rating curves are available, the present approach may yield superior forecasts. Since in practice the accuracy of the employed rating curves, used to convert stage measurements into discharge values for flow routing, may be somewhat uncertain, application of the present technique is recommended for rating-curve falsification. The method allows for stage predictions using physically based flow routing in rivers where flow rates are unknown or the available rating curves are inaccurate. The technique can also be used without modification for streams with tributaries.

© 2005 Elsevier B.V. All rights reserved.

*Keywords:* Stream-flow; Flow routing; Forecasting; Hydrologic model; Rating curve; State-space; Cascade model

## 1. Introduction

The Saint-Venant equations (continuity and momentum) of open channel flow define a system of distributed parameters where the dependent variable, flow rate, is a continuous function of distance along the channel, in addition to time. In practical applications, information of channel properties is

available at certain locations only, requiring the transformation of the partial differential equations into either ordinary or algebraic equations, which describe the flow at specified cross-sections of the channel. This entails a lumped parameter system of flow routing in place of the original distributed parameter one, where now the dependent variable is only a continuous function of time. A great majority of the flow routing methods are based on the kinematic wave equation, the latter being a first-order approximation of the momentum equation. The Kalinin–Milyukov–Nash (KMN) cascade (Kalinin and Milyukov, 1957; Nash, 1957) is such a linear flow routing approach, whose discretized version using a pulse-, and subsequently, a sample-data

\* Corresponding author. Tel.: +1 402 472 9667; fax: +1 402 472 4608.

E-mail address: [jszilagy1@unl.edu](mailto:jszilagy1@unl.edu) (J. Szilagyi).

<sup>1</sup> On leave from the Conservation and Survey Division, University of Nebraska-Lincoln, 113 Nebraska Hall, Lincoln, NE 68588-0517, USA.

system framework were presented by Szöllősi-Nagy (1982) and Szilagyi (2003), respectively, both in a state-space formulation.

The state-space description of the linear kinematic wave equation (with no lateral inflow)

$$\begin{aligned} \frac{\partial Q(l,t)}{\partial t} + C \frac{\partial Q(l,t)}{\partial l} &= 0 \\ Q(0,t) &= Q_0(t) \\ Q(l,t) &\neq \infty, \text{ as } l \rightarrow \infty, t \geq 0 \end{aligned} \tag{1}$$

where  $Q[L^3T^{-1}]$  is discharge,  $C[LT^{-1}]$  is wave celerity,  $l$  and  $t$  are spatial and temporal coordinates, respectively; can be obtained by applying a backward difference-scheme for the spatial derivative

$$\begin{aligned} \frac{dQ(l_j,t)}{dt} &= -C \frac{Q(l_j,t) - Q(l_{j-1},t)}{\Delta l} \\ &= \frac{C}{\Delta l} Q(l_{j-1},t) - \frac{C}{\Delta l} Q(l_j,t) \quad 1 \leq j \leq n \end{aligned} \tag{2}$$

Introducing the state variable  $\mathbf{x}$  of the flow-rate values of  $n$  serially connected subreaches (Fig. 1)

$$\mathbf{x}(t) = \begin{bmatrix} Q(l_1,t) \\ Q(l_2,t) \\ \vdots \\ Q(l_n,t) \end{bmatrix} \tag{3}$$

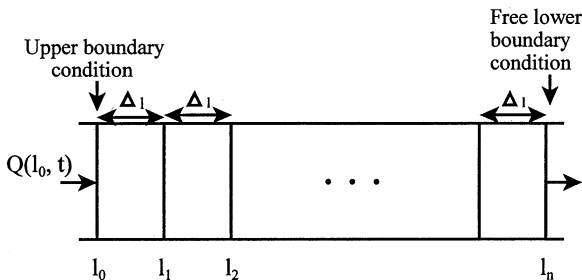


Fig. 1. Spatial discretization of the linear kinematic wave equation.

and having  $u(t) = Q_0(t) = Q(l_0,t)$ , one can write

$$\begin{aligned} \begin{bmatrix} \dot{Q}(l_1,t) \\ \dot{Q}(l_2,t) \\ \vdots \\ \dot{Q}(l_n,t) \end{bmatrix} &= \frac{C}{\Delta l} \begin{bmatrix} -1 & & & 0 \\ & 1 & -1 & \\ & & \ddots & \ddots \\ & & & 1 & -1 \end{bmatrix} \begin{bmatrix} Q(l_1,t) \\ Q(l_2,t) \\ \vdots \\ Q(l_n,t) \end{bmatrix} \\ &+ \begin{bmatrix} \frac{C}{\Delta l} \\ 0 \\ \vdots \\ 0 \end{bmatrix} u(t) \end{aligned} \tag{4a}$$

or in a more succinct form as

$$\dot{\mathbf{x}}(t) = \mathbf{F}\mathbf{x}(t) + \mathbf{G}u(t) \tag{4b}$$

which is the state equation of a linear, time-invariant continuous dynamic system (Szöllősi-Nagy, 1982). Discharge from the last subreach is the flow rate,  $y(t)$ , of the whole reach

$$y(t) = [0, 0, \dots, 1] \begin{bmatrix} Q(l_1,t) \\ \vdots \\ Q(l_n,t) \end{bmatrix} \tag{5a}$$

or

$$y(t) = \mathbf{H}\mathbf{x}(t) \tag{5b}$$

The KMN-cascade results by considering each subreach as a linear storage element having the property

$$Q(t) = \frac{1}{K} s(t) \tag{6}$$

where  $s[L^3]$  is water volume in storage within the element, and  $K[T]$  is the mean residence time of it. The inverse of the mean residence time,  $k=K^{-1}$ , is called the storage coefficient of the linear storage element.

By expressing the storage coefficient,  $k$ , with  $C/\Delta l$ , and again considering  $n$  serially connected

subreaches, the substitution of Eq. (6) into Eq. (4a) yields

$$\begin{bmatrix} \dot{s}_1(t) \\ \dot{s}_2(t) \\ \vdots \\ \dot{s}_n(t) \end{bmatrix} = \begin{bmatrix} -k & & & 0 \\ k & -k & & \\ & & \ddots & \\ 0 & & & k & -k \end{bmatrix} \begin{bmatrix} s_1(t) \\ s_2(t) \\ \vdots \\ s_n(t) \end{bmatrix} + \begin{bmatrix} 1 \\ 0 \\ \vdots \\ 0 \end{bmatrix} u(t) \tag{7a}$$

or in matrix notation

$$\dot{\mathbf{s}}(t) = \mathbf{F}^* \mathbf{s}(t) + \mathbf{G}^* u(t) \tag{7b}$$

with the output equation defined as

$$y(t) = [0, 0, \dots, k] \begin{bmatrix} s_1(t) \\ \vdots \\ s_n(t) \end{bmatrix} \tag{8a}$$

or

$$y(t) = \mathbf{H}^* \mathbf{s}(t) \tag{8b}$$

The two linear systems defined by Eqs. (4b), (5b), (7b), and (8b), are equivalent, since their impulse responses are the same (Szöllősi-Nagy, 1989; Desoer, 1970) through the  $k = C/\Delta l$  substitution.

An interesting property of the two systems must be mentioned here that makes them effective tools of flow routing. The spatial discretization introduces an artificial diffusion (Cunge, 1969) into the system equations and so enables them to account for diffusional processes and thus approximate the solution of the linear diffusion wave equation, the latter itself a second-order approximation of the momentum equation (Szöllősi-Nagy, 1989)

$$\frac{\partial Q(l, t)}{\partial t} + C \frac{\partial Q(l, t)}{\partial l} = D \frac{\partial^2 Q(l, t)}{\partial l^2} \tag{9}$$

where  $D[L^2T^{-1}]$  is a constant. Because the discrete KMN-cascade of Eqs. (7b) and (8b) is equivalent to Eqs. (4b) and (5b) from a systems point of view, and the latter being a special discretized form of the linear kinematic wave equation, these authors consider the discrete KMN-cascade a physically based flow routing technique.

Below it is demonstrated how the KMN-cascade can be formulated for flow routing when flow-rate

information is absent. Considering that for larger streams and for rivers the primary source of flow information is in the form of stage measurements, such an approach may especially prove useful. These stage measurements are converted into instantaneous flow rates through the application of an established rating curve for the channel cross-section in question. It should be noted that all flow routing techniques assume negligible backwater effects in the stream as well as an essentially single-valued rating curve (Fread, 1993).

## 2. Model description

The linear storage equation (Eq. (6)) results if one assumes that the exponent ( $\alpha$ ) is the same in the functional relationships between flow rate and stage as well as between water stored in a channel reach and stage

$$Q(t) = c_1[H(t) + a]^\alpha \tag{10a}$$

$$s(t) = c_2[H(t) + a]^\alpha \tag{10b}$$

where  $H[L]$  is the measured value of stage above or below datum, and  $c_1 [L^{3-\alpha}T^{-1}]$ ,  $c_2 [L^{3-\alpha}]$ , and  $a [L]$  are constants. Dividing Eq. (10a) by (10b) yields

$$Q(t) = \frac{c_1}{c_2} s(t) = ks(t) \tag{11}$$

Inserting Eqs. (10a), (10b), and (11) into the lumped continuity equation of the channel reach

$$\dot{s}(t) = Q_1(t) - Q_2(t) = Q_1(t) - ks(t) \tag{12a}$$

results in

$$\begin{aligned} c_2 \alpha [H_2(t) + a]^{\alpha-1} \frac{dH_2(t)}{dt} \\ = -\frac{c_1}{c_2} c_2 [H_2(t) + a]^\alpha + c_3 [H_1(t) + b]^\beta \end{aligned} \tag{12b}$$

where the subscripts 1 and 2 refer to the up- and downstream ends of the channel reach, and  $c_3 [L^{3-\beta}T^{-1}]$ ,  $b [L]$ , and  $\beta$  are constants of the stage-discharge relationship of the upstream location.

By rearranging Eq. (12b) one obtains

$$\frac{dH_2(t)}{dt} = -\frac{c_1}{c_2\alpha} [H_2(t) + a] + \frac{c_3}{c_2\alpha} \frac{[H_1(t) + b]^\beta}{[H_2(t) + a]^{\alpha-1}} \tag{13}$$

which shows that in general the future outflow rate of the reach is determined by a certain combination of in- and outflow rates through the last term of the right-hand-side of the equation. However, by assuming that both exponents are unity, Eq. (13) simplifies into

$$\begin{aligned} \frac{dH_2(t)}{dt} &= -\frac{c_1}{c_2} H_2(t) + \frac{c_3}{c_2} H_1(t) + c_4 \\ &= -kH_2(t) + cH_1(t) + c_4 \end{aligned} \tag{14a}$$

where  $c=c_3/c_2$  [ $T^{-1}$ ], and  $c_4$  [ $LT^{-1}$ ] are other constants. In comparison with Eq. (12a) or (7a), the constant multiplier of  $H_1$  and an additional constant value now are of no concern because linearity assures that the output is proportional to any constant multiplier in the input values, and the presence of a constant input means only an additional constant value in the output values after an initial spin-up period. Because of the arbitrary reference points in the stage measurements of differing locations, routed upstream stage values have to be scaled up or down in any case to match the measured downstream stage values, thus the presence of a constant multiplier (and an additional constant) in the input stage values means no extra scaling. Consequently  $c$  and  $c_4$  can be chosen arbitrarily. In this way, Eq. (14a) can be expressed as

$$\frac{dH_2(t)}{dt} = -kH_2(t) + H_1(t) \tag{14b}$$

which now is of the same form as Eq. (7a) of the KMN-cascade when written for a single subreach.

The reason why the required scaling is not typically a linear function stems from the general nonlinear shape of the actual rating curves whereas in the derivation of Eq. (14b) linear rating curves were employed. The required scaling of routed to observed stage values can be achieved by the application of a polynomial curve fitting in the form of

$$\begin{aligned} \widehat{H}_2^{sc}(t) &= p_1 \widehat{H}_2^m(t) + p_2 \widehat{H}_2^{m-1}(t) + \dots \\ &+ p_m \widehat{H}_2(t) + p_{m+1} \end{aligned} \tag{15}$$

where  $\widehat{H}_2^{sc}$  is the scaled,  $\widehat{H}_2$  is the original model estimate of the downstream stage value, and the  $p_i$ s [ $L^{i-m}$ ] are the constant coefficients of the polynomial of a predefined order  $m$ .

With these considerations the solution of the KMN-cascade model can be applied. Szilagyi (2003) derived the solution of Eq. (7b) for a sample-data system which implies that the stage measurements are available only at discrete time intervals ( $\Delta t$ ) with an assumed linear change in the values between consecutive discrete samples. Applying the solution to Eq. (14b) over  $n$  serially connected subreaches one obtains

$$\begin{aligned} \mathbf{H}(t + \Delta t) &= \mathbf{\Phi}(\Delta t)\mathbf{H}(t) + \mathbf{\Gamma}_1(\Delta t)H_1(t + \Delta t) \\ &+ \mathbf{\Gamma}_2(\Delta t)H_1(t) \end{aligned} \tag{16}$$

where the vector  $\mathbf{H}$  comprises the modeled stage values of the  $n$  subreaches, the  $\mathbf{\Phi}(\Delta t)$  state-transition matrix, and the  $\mathbf{\Gamma}_1(\Delta t)$  and  $\mathbf{\Gamma}_2(\Delta t)$  input-transition vectors are defined as (Szilagyi, 2003)

$$\mathbf{\Phi}(\Delta t) = \begin{bmatrix} e^{-\Delta tk} & 0 & 0 & \dots & 0 \\ \Delta tke^{-\Delta tk} & e^{-\Delta tk} & 0 & \dots & 0 \\ \frac{(\Delta tk)^2}{2!}e^{-\Delta tk} & \Delta tke^{-\Delta tk} & e^{-\Delta tk} & 0 & \vdots \\ \vdots & \vdots & \ddots & \ddots & 0 \\ \frac{(\Delta tk)^{n-1}}{(n-1)!}e^{-\Delta tk} & \frac{(\Delta tk)^{n-2}}{(n-2)!}e^{-\Delta tk} & \dots & \Delta tke^{-\Delta tk} & e^{-\Delta tk} \end{bmatrix} \tag{17}$$

$$\Gamma_1(\Delta t) = \begin{bmatrix} \frac{1}{k} \frac{\Gamma(1, \Delta tk)}{\Gamma(1)} \left[ 1 + \frac{e^{-\Delta tk}}{\Gamma(1, \Delta tk)} - \frac{1}{\Delta tk} \right] \\ \frac{1}{k} \frac{\Gamma(2, \Delta tk)}{\Gamma(2)} \left[ 1 + \frac{(\Delta tk)e^{-\Delta tk}}{\Gamma(2, \Delta tk)} - \frac{2}{\Delta tk} \right] \\ \vdots \\ \frac{1}{k} \frac{\Gamma(n, \Delta tk)}{\Gamma(n)} \left[ 1 + \frac{(\Delta tk)^{n-1}e^{-\Delta tk}}{\Gamma(n, \Delta tk)} - \frac{n}{\Delta tk} \right] \end{bmatrix} \quad (18)$$

and

$$\Gamma_2(\Delta t) = \begin{bmatrix} \frac{1}{k} \frac{\Gamma(1, \Delta tk)}{\Gamma(1)} \left[ \frac{1}{\Delta tk} - \frac{e^{-\Delta tk}}{\Gamma(1, \Delta tk)} \right] \\ \frac{1}{k} \frac{\Gamma(2, \Delta tk)}{\Gamma(2)} \left[ \frac{2}{\Delta tk} - \frac{(\Delta tk)e^{-\Delta tk}}{\Gamma(2, \Delta tk)} \right] \\ \vdots \\ \frac{1}{k} \frac{\Gamma(n, \Delta tk)}{\Gamma(n)} \left[ \frac{n}{\Delta tk} - \frac{(\Delta tk)^{n-1}e^{-\Delta tk}}{\Gamma(n, \Delta tk)} \right] \end{bmatrix} \quad (19)$$

The output equation now becomes

$$\widehat{H}_2(t) = [0, 0, \dots, 1] \begin{bmatrix} H_1(t) \\ \vdots \\ H_n(t) \end{bmatrix} \quad (20)$$

the term on the left-hand-side being the input to Eq. (15). For channel reaches with tributaries, stages are routed separately between up- and downstream stations on the main channel and the upstream station of each tributary and the downstream station of the main channel due to linearity of the KMN-cascade, before inserting the  $\widehat{H}_2(t)$  ( $j=1, \dots, T+1$ , where  $T$  is the number of tributaries within the reach) values into Eq. (15). Then the  $p_i$  ( $i=1, \dots, m$ ) coefficients of the polynomial become vector-valued.

As a practical consideration it can be mentioned that  $c_4$  in Eq. (14a) may need to be chosen different from zero in order to avoid negative values in the routing of stages when the upstream stage value can drop below datum.

### 3. Model application and conclusions

The above model was tested on three rivers in Hungary: the Danube, its tributary, the Tisza River,

Table 1

Stream reaches used in the study with corresponding reach lengths  $L$  (km), average channel slopes  $I$  (%), as well as drainage areas  $D$  (km<sup>2</sup>) belonging to the downstream stations

	$L$	$D$	$I$
Nagymaros–Budapest	48.1	184,893	0.0071
Budapest–Dunaujvaros	65.9	188,273	0.0090
Budapest–Paks	115.2	189,092	0.0091
Paks–Baja	52.6	208,282	0.0065
Baja–Mohacs	31.8	209,064	0.0058
Tiszabercel–Tokaj	25.9	49,849	0.0096
Sarospatak–Tokaj	37.1	13,000 <sup>a</sup>	0.0114
Arad–Mako	72.7	30,149	0.0057

<sup>a</sup> Drainage area of the tributary (Bodrog) above the confluence.

and a tributary of the Tisza, the Maros River. See Table 1 for a list of gaging stations with corresponding drainage areas and mean channel slopes. Model results were compared with that of an operative, real-time hydrological forecasting version of the KMN-cascade using actual rating-curve-derived discharge values. The operational model uses a time-step of  $\Delta t=12$  h and employs a multilinear approach (Becker and Kundzewicz, 1987; Szolgay, 1991) where discharges are routed through parallel cascades of linear storages representing low-, and mean-flow channel as well as flood conditions over the floodplain, thus creating a nonlinear model. The operative model has  $3 \times 2=6$  ( $n$  and  $k$  values for each three cascades) parameters, plus a one-step autoregressive coefficient for prediction error updating while the proposed model has two, plus one autoregressive (ar), parameters and is run with a time-step of  $\Delta t=24$  h. To assure identical input values for model performance comparisons, the new model uses forecasted stage values of a lead-time of 24 h, calculated by the operative model for the upstream stations. Both models were run in a continuous error-updating mode, which means that each forecast value is modified by a certain percentage (given by the value of the autoregressive parameter) of the previous day’s model error prior to error updating.

Fig. 2 displays the location of the gaging stations used by the models. The corresponding rating curves, required by the operative model, are displayed in Fig. 3.

Parameters of the proposed model were optimized with 2 years of data from the period January 1, 2000 to

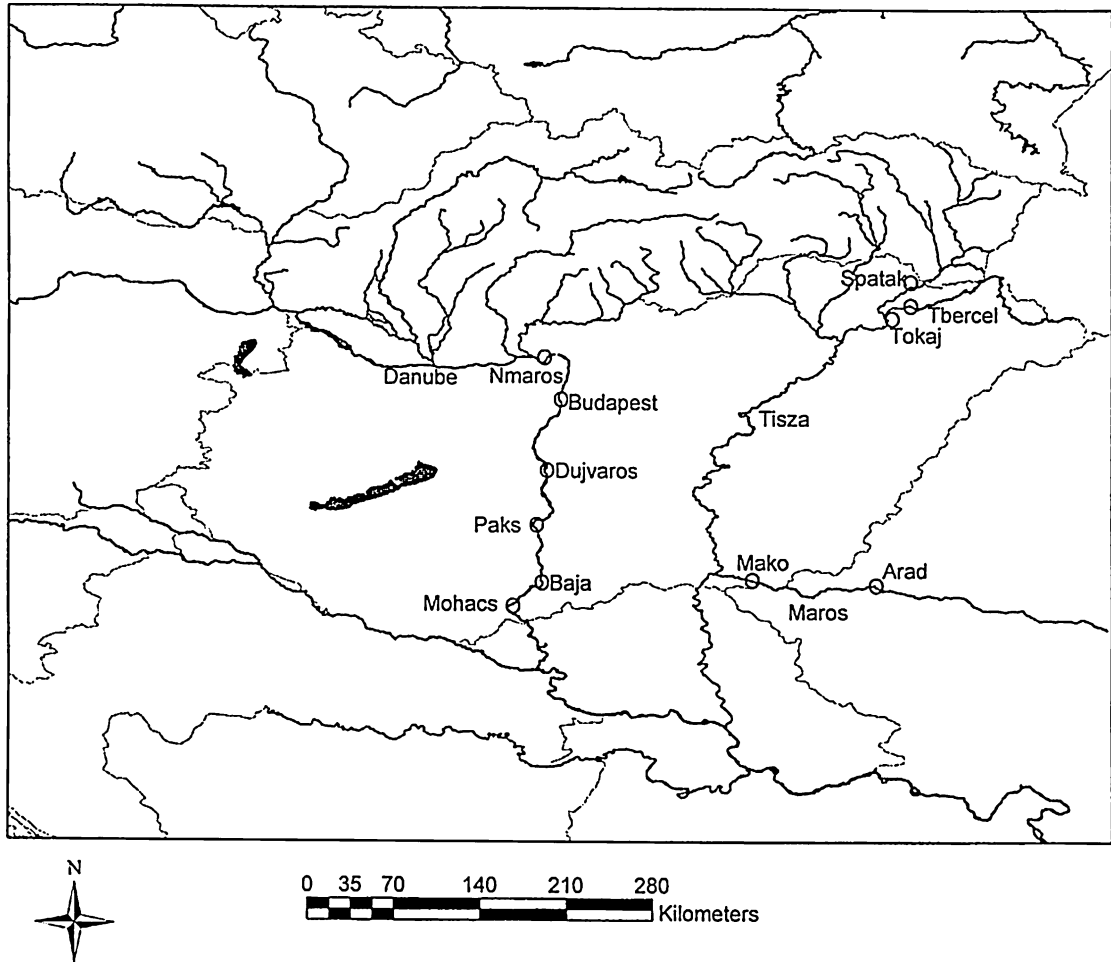


Fig. 2. Spatial locations of the gaging stations used in the study.

December 31, 2001. Model results, using the optimized parameter values, were compared with operative model outputs for the period January 1, 2002–September 18, 2003. Model performance was assessed by two statistics: the mean root-square error ( $\sigma$ ) and a Nash–Sutcliffe-type efficiency coefficient (NSC) which is defined as

$$\text{NSC} = 100 \left( 1 - \frac{\sum_i (\hat{H}_i - H_i)^2}{\sum_i (H_{i-1} - H_i)^2} \right) \quad (\%) \quad (21)$$

where  $\hat{H}_i$  is the predicted, and  $H_i$  the observed stage value on day  $i$ . The closer is the NSC value to 100% the better are the predictions. Note that the NSC value may be negative when the forecasts are worse than

the naive prediction (see denominator), which takes the stage value of the actual day as the one-day forecast. Table 2 lists the optimized model parameter values. Optimization of the  $n$ ,  $k$ , and  $ar$  values of the proposed model was carried out by a systematic trial-and-error search where trial values of the parameters were chosen from ever-decreasing predefined ranges of the parameters with ever-increasing corresponding resolution terminating at a chosen set resolution. Parameters of the nonlinear regression equation (Eq. (15)) were obtained using the Matlab function ‘Nlinfit’ for the multivariate case, and the function ‘Polyfit’ for the univariate case, both by prescribing a third-order polynomial.

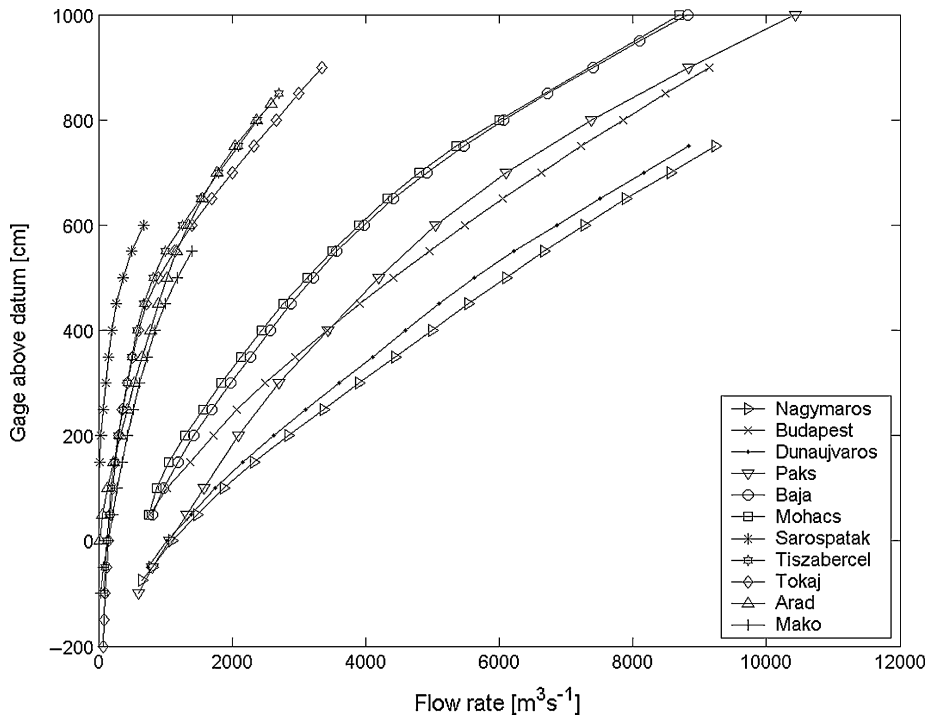


Fig. 3. Rating curves used by the operative model.

Fig. 4 displays the unscaled (i.e. before the application of Eq. (15)) forecasts against observed stages of the Danube at Baja. Application of assumed linear rating curves instead of more realistic measured ones (Fig. 3) causes the curvature of the best-fit polynomial at large values. Such a systematic error, however, can be easily corrected via Eq. (15). Fig. 5 displays the so-scaled forecasts, which now scatter around the 1:1 line. Continuous error updating further reduces this scatter (Fig. 6) resulting in the one-day stage forecasts of Fig. 7 for the verification period. Note that the first few forecast values may be off mark, due to the spin-up period required for the output values to adjust for the constant shift in the input stage values between Eqs. (14a) and (14b) and due to the fact that modeling starts with an arbitrary zero initial value of the **H** vector. Consequently, the first four forecast values were left out from all subsequent analysis. Table 3 lists the performance statistics of the one-day model predictions of both the operative and the proposed models for the two distinct periods. Based on Table 3 it can be stated that the proposed

model has stable optimized parameter values since model performance deteriorates only slightly between the two periods. During the verification period there happened to be a major, but a relatively short-term (several days) water release through a dam of the Tisza downstream of Tokaj which contributed to a large drop in model efficiencies between the periods.

In general, physically based models are expected to have more stable parameters in time than so-called

Table 2  
Optimized model parameter values for different stream reaches

	Optimization period
Nagymaros–Budapest	$k = 11 \text{ (day}^{-1}\text{)}, n = 4, ar = 0.2$
Budapest–Dunaujvaros	$k = 6.8 \text{ (day}^{-1}\text{)}, n = 4, ar = 0.2$
Budapest–Paks	$k = 3.9 \text{ (day}^{-1}\text{)}, n = 4, ar = 0.6$
Paks–Baja	$k = 3.2 \text{ (day}^{-1}\text{)}, n = 2, ar = 0.8$
Baja–Mohacs	$k = 2.7 \text{ (day}^{-1}\text{)}, n = 1, ar = 0.7$
Tiszabercel–Tokaj	$k = 8.5 \text{ (day}^{-1}\text{)}, n = 1, ar = 0.9$
Sarospatak–Tokaj	$k_{trib} = 1.5 \text{ (day}^{-1}\text{)}, n_{trib} = 2$
Arad–Mako	$k = 14.5 \text{ (day}^{-1}\text{)}, n = 7, ar = 1$

The subscript ‘trib’ refers to the tributary (Bodrog River) of the Tisza.

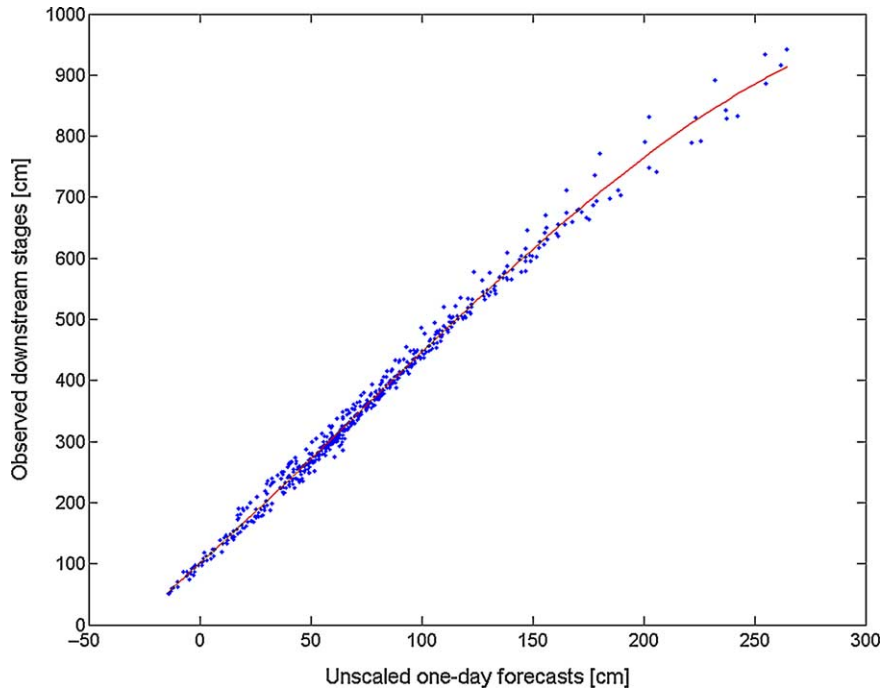


Fig. 4. Observed stages at Baja versus unscaled one-day forecasts of the verification period.

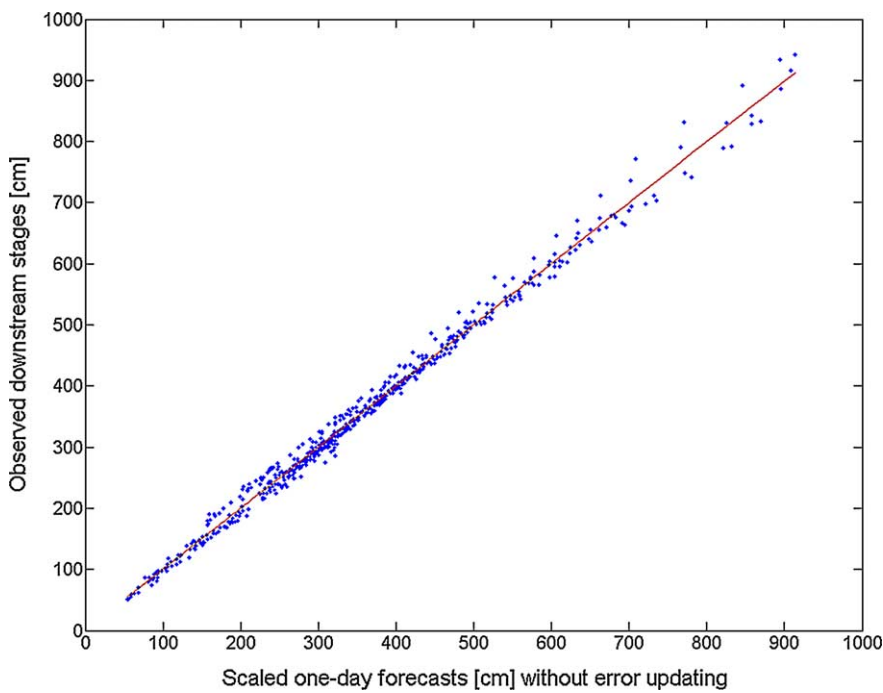


Fig. 5. Observed stages at Baja (verification period) versus scaled one-day forecasts with no error updating.

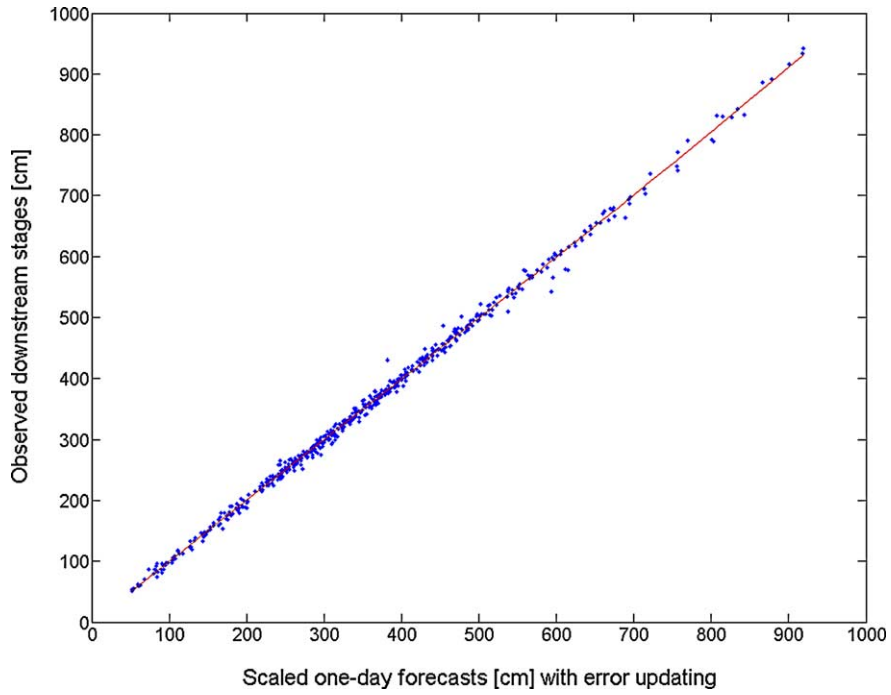


Fig. 6. Observed stages at Baja (verification period) versus scaled one-day forecasts with error updating.

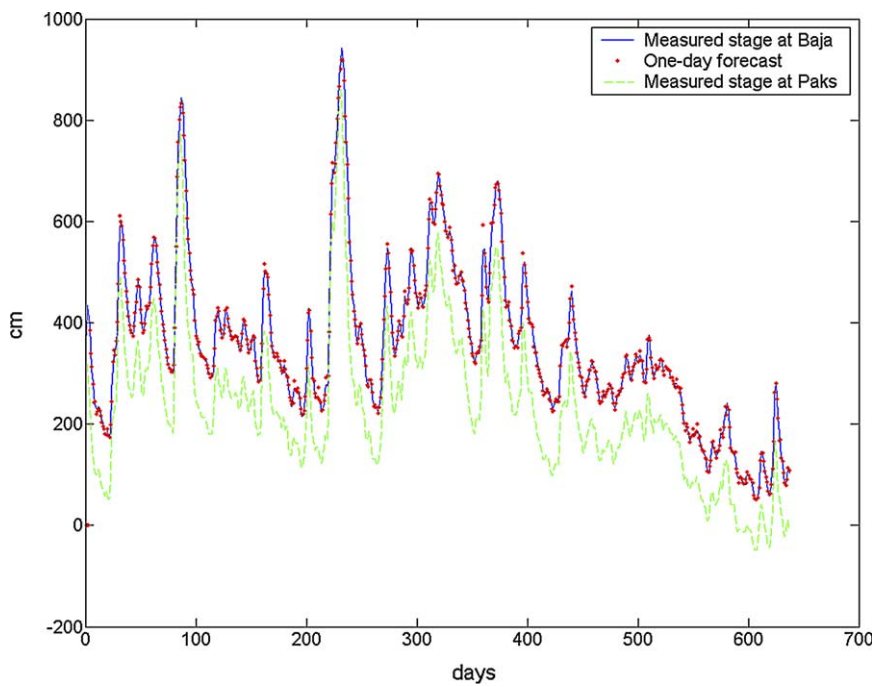


Fig. 7. Observed stages at Paks and Baja (verification period) with the one-day forecasts shown.

Table 3  
Model performance statistics of the one-day ahead stage forecasts

Optimization period	
Budapest	$\sigma = 5.95(5.67)$ (cm), NSC = 94.21(94.75)%
Dunaujvaros	$\sigma = 6.58(8.42)$ (cm), NSC = 92.15 (87.14)%
Paks	$\sigma = 5.08(7.46)$ (cm), NSC = 92.67(91.96)%
Baja	$\sigma = 6.92(5.68)$ (cm), NSC = 91.75(94.43)%
Mohacs	$\sigma = 5.28(5.49)$ (cm), NSC = 94.34(93.90)%
Tokaj	$\sigma = 6.23(8.53)$ (cm), NSC = 78.87(60.34)%
Mako	$\sigma = 12.02(11.85)$ (cm), NSC = 66.79(67.72)%
Verification period	
Budapest	$\sigma = 8.11(7.83)$ (cm), NSC = 91.66(92.23)%
Dunaujvaros	$\sigma = 8.59(9.88)$ (cm), NSC = 89.13(85.75)%
Paks	$\sigma = 6.07(9.46)$ (cm), NSC = 95.70(89.55)%
Baja	$\sigma = 7.69(7.87)$ (cm), NSC = 91.81(91.45)%
Mohacs	$\sigma = 6.16(6.72)$ (cm), NSC = 93.79(92.61)%
Tokaj	$\sigma = 9.72(17.57)$ (cm), NSC = 44.76(0)%
Mako	$\sigma = 9.36(10.85)$ (cm), NSC = 64.01(51.49)%

The values in parentheses refer to the operative model.

black-box models (Szöllősi-Nagy, 1989) and also more accurate forecasts with increasing lead-times (Szöllősi-Nagy, 1989; Szilagyi, 1992). Because the former (may they be very simplified) give some insight into the physical processes involved, temporal changes in parameter values can often be linked to changes in the channel or floodplain conditions, such as conveyance. Also, model transferability of physically based models between gaged and ungaged basins is typically better than that of black-box models (Nash and Sutcliffe, 1970) simply because model parameter values can be linked to measurable basin properties. In our case, the ratio of optimized values of  $n$  and  $k$  yields the mean travel time of flow propagation for the given reach. Since this latter is a function of channel properties mainly, initial guesses of the  $n$  and  $k$  values for a new, ungaged stream can be obtained by using such information only.

Overall, performance of the proposed model is very similar to that of the operative model (Table 3). For certain stations (Budapest, Baja, and Mako) the operative model produces more accurate predictions than the proposed model. This is what would normally be expected, since the operative model uses extra information (i.e. known rating curves) for flow routing. One plausible explanation of why the proposed model may perform better than the operative one for other stations (Dunaujvaros, Paks, and Tokaj) can be that for those stations the rating curves may not be accurate

enough or they may be outdated, i.e. they do not reflect correctly the channel and flow conditions of the modeled periods. Suboptimal parameter values (which could stem from a higher number of parameters to be optimized, i.e. 7 as opposed to 3) in the case of the operative model might also explain its underperformance, but it is unlikely knowing that parameter values of the operative model are updated each day using information from the previous 90 days (Szilagyi, 1992). Here, it should be emphasized that the proposed model is not meant for replacing models that use measured rating-curve information. Whenever reliable rating curves are available, a flow-rate formulation, i.e. Eq. (7a), should always be preferred over a stage formulation, Eq. (14b). However, an additional (on top of flow rates) flow routing using stages only, can detect inadequacies in the data required by the former. Naturally, when no information of rating curves is available, the proposed model (or its variant, such as the multilinear formulation) may easily be a proper candidate of a physically based model to apply. Szilagyi (2004) provides an exhaustive list of the advantages of applying a state-space approach of flow routing over a numerical solution of Eq. (1) or (9) beyond the already-mentioned properties that flow routing is a lumped parameter approach while the kinematic and diffusion wave equations are distributed ones.

## Acknowledgements

The authors are grateful to K.M. O'Connor and D.A. Hughes for their valuable comments on the manuscript.

## References

- Becker, A., Kundzewicz, Z.W., 1987. Nonlinear flood routing with multilinear models. *Water Resour. Res.* 23 (6), 1043–1048.
- Cunge, J.A., 1969. On the subject of flood propagation computation method (Muskingum method). *J. Hydraul. Res.* 7 (2), 205–230.
- Doer, C.A., 1970. Notes for a Second Course on Linear Systems. van Nostrand, New York.
- Fread, D.L., 1993. Flow routing. In: Maidment, D.R. (Ed.), *Handbook of Hydrology*. McGraw-Hill, New York.

- Kalinin, G.P., Milyukov, P.I., 1957. O raschete neustanovivshego-sya dvizheniya vody v otkrytykh ruslakh (on the computation of unsteady flow in open channels). *Met. Gydrol. Z.* 10, 10–18 (Leningrad).
- Nash, J.E., 1957. The form of instantaneous unit hydrograph. *Int. Assoc. Sci. Hydrol. Publ.* 45 (3), 114–121.
- Nash, J.E., Sutcliffe, J.V., 1970. River flow forecasting through conceptual models part I—A discussion of principles. *J. Hydrol.* 10, 282–290.
- Szilagyi, J., 1992. Stage forecasting by an adaptive, stochastic model (In Hungarian: Vízállások előrejelzése adaptív, sztochasztikus modellel). *Vizügyi Közlemények* 74 (1), 91–104.
- Szilagyi, J., 2003. State-space discretization of the Kalinin–Milyukov–Nash cascade in a sample-data system framework for streamflow forecasting. *J. Hydrol. Eng.* 8 (6), 339–347.
- Szilagyi, J., 2004. Accounting for stream–aquifer interactions in the state-space discretization of the KMN-cascade for streamflow forecasting. *J. Hydrol. Eng.* 9 (2), 135–143.
- Szolgay, J., 1991. Prediction of river runoff changes due to hydropower development on the Danube at Gabčíkovo. *IAHS Publ.* 201, 209–218.
- Szöllősi-Nagy, A., 1982. The discretization of the continuous linear cascade by means of state space analysis. *J. Hydrol.* 58, 223–236.
- Szöllősi-Nagy, A., 1989. Real-Time Streamflow Forecasting using Dynamically Structured Deterministic-Stochastic Models (In Hungarian: A Mederbeli Lefolyás Real-Time Előrejelzése Dinamikus Strukturális-Sztochasztikus Modellekkel). VITUKI, Budapest.